Extended Abstracts of the 2014 International Conference on Solid State Devices and Materials, Tsukuba, 2014, pp534-535

Epitaxial Growth, Doping, and Electron Transport of the Semiconducting Oxides In_2O_3, Ga_2O_3, and SnO_2

Oliver Bierwagen[1,2], Mark E. White[2], Min-Ying Tsai[2] , James S. Speck[2], Takahiro Nagata[3], Natalie Preissler[1], Patrick Vogt[1]

[1] Paul-Drude-Inst. für Festkörperelektronik
Hausvogteiplatz 5—7
10117 Berlin, Germany
Phone: +49-30-20377-491 E-mail: bierwagen@pdi-berlin.de
[2] Univ. of California
Santa Barbara, CA 93106, USA
[3] National Inst. for Materials Sci.
1—1 Namiki, Tsukuba, Ibaraki 305-0044, Japan

Abstract

The growth of high-quality, single-crystalline SnO_2, In_2O_3, and Ga_2O_3 films by plasma assisted molecular beam epitaxy is presented. The growth-related issues faceting, nucleation, and sub-oxide formation are discussed. The resistivity of SnO_2 and In_2O_3 was systematically varied from semi-insulating to highly conductive behavior by donor and (deep)acceptor doping. Realization of *p*-type conductivity seems to be hard or impossible. The influence of the surface electron accumulation layer on conductivity, its control, and its impact on contacts will be described. With the example of In_2O_3 the influence of intrinsic defects on transport properties will be demonstrated.

1. Introduction

Semiconducting oxides are playing a growing role as active device material in (opto)electronic devices. Application in transparent electronics, power electronics, or photo-detectors requires a semiconductor-like material quality in contrast the low material quality sufficient for the conventional transparent contact applications of these oxides.

This study investigates the growth of high-quality semiconducting oxide layers, their conductivity and its control, and their contact and transport properties relevant for device applications.

2. Experiment

Plasma assisted molecular beam epitaxy (PAMBE) was used to grow SnO_2, In_2O_3, and Ga_2O_3 layers with high crystal quality and purity, and with well-defined transport properties by systematic donor and (deep) acceptor doping [1]. Resistivity, Hall, and Seebeck coefficient measurements were used to investigate the transport properties of the grown films. Annealing in different atmospheres was used to alter the (compensating) intrinsic defect concentration in In_2O_3. Current-voltage measurements with different contact metals were used to investigate contact properties, and XPS measurements identified the presence/absence of surface accumulation layers. Surface treatments with an oxygen plasma helped depleting the surface accumulation.

3. Results and discussion

3.1 Growth

Due to the absence of native substrates, growth was performed by heteroepitaxy on foreign subtrates, i.e. r-plane Al_2O_3 for single crystalline rutile SnO_2(101) and ZrO_2:Y(001) [YSZ(001)] for single crystalline cubic In_2O_3(001). Ga_2O_3 was grown on c-plane Al_2O_3 (with rotational domains) and on single crystalline on beta-Ga_2O_3(100). The recent availability of native oxide substrates for all semiconducting oxides investigated in this work will lead to a further improvement in crystal quality.

The formation and sublimation of volatile, parasitic suboxides for SnO_2 [2] and Ga_2O_3 [3] results in a decreasing growth rate in the metal-rich growth regime.

For In_2O_3, the anisotropy of the surface free energy leads to the preferential formation of {111}-facetted surfaces for the growth of (001)-oriented In_2O_3 (Fig.1, top), whereas (111)-oriented In_2O_3 formed smooth surfaces. Metal-rich growth conditions were able to lower the In_2O_3 (001) surface free energy enabling the growth of smooth, unfacetted In_2O_3 (001) layers (Fig.1, bottom) [4].

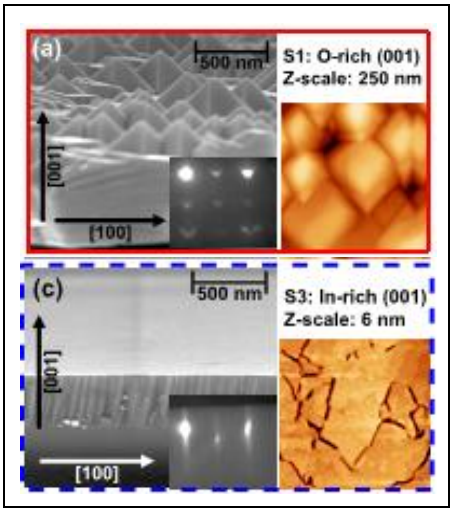

Fig. 1 Morphology of In_2O_3 films grown on YSZ(001) under oxygen-rich conditions (top) and inium-rich conditions (bottom).

In_2O_3 grows in a Volmer-Weber growth mode on YSZ(001), resulting in suppressed nucleation on the substrate and formation of micron-sized islands. Reduced substrate temperature or increased oxygen flux helped enhancing the nucleation to obtain continuous films by fast coalescence of densely packed nuclei [5]. Depending on application, suppressed wetting can be used to produce oxide islands, faceting can help defining the surface properties (e.g. for chemical sensors), and enhanced nucleation and prevented faceting helps to obtain smooth, continuous films that are required for most technological applications.

Systematic doping was studied for SnO_2 by the donor Sb [6] and the (deep)acceptors In [7] and Ga [8], and for In_2O_3 by the donor Sn [9] and the (deep)acceptor Mg [10]. Doping limits were identified by the formation of secondary crystalline phases [1, 9, 10], and Sn-incorporation into In_2O_3 was inhibited at high Sn-concentrations --- likely due to the preferential formation of parasitic Sn-suboxides [9]. High Sn-doping prevented the {111} faceting and enhanced the nucleation on YSZ [9].

3.2 Electron transport in SnO_2 and In_2O_3

Similar to most *n*-type transparent semiconducting oxides, SnO_2 and In_2O_3 are *n*-type conductive even in the absence of intentional donors --- they are unintentionally doped (UID). Our UID SnO_2 [6] and In_2O_3 [11] films showed electron concentrations due to shallow donors on the order of $10^{17}cm^{-3}$ at electron mobilities of ~100 and ~200 cm^2/Vs, respectively.

A surface electron accumulation layer was present in both oxides [13,14], which enhanced the formation of ohmic contacts [12] but prevented the formation of Schottky contacts [12—15]. A surface oxygen plasma treatment was able to deplete the accumulation [13, 14] and enable formation of Schottky contacts [12, 15]. Unlike in e.g. InN, the conductance contribution to the UID conductivity was negligible in both oxides [8, 14].

The resistivity of both oxides could be varied by doping over nine orders of magnitude from the highly conductive to the semi-insulating regime (Fig.2). Systematic Sb-doping of SnO_2 was performed for concentrations from 10^{18} to $2.6x10^{20}cm^{-3}$ with high doping efficiency achieving a TCO-like conductivity [6] whereas acceptor doping with In and Ga allowed to make the SnO_2 semi-insulating [7,8] but not *p*-type conductive. At acceptor concentrations in excess of $\sim10^{20}cm^{-3}$ the SnO_2 *n*-type conductivity of SnO_2 increased again.

Systematic donor doping of In_2O_3 with Sn allowed to achieve electron concentrations of $>10^{21}cm^{-3}$ and a resistivity of 10^{-4} Ohm cm [9]. Doping by Mg allowed to achieve semi-insulating In_2O_3 but no *p*-type conductivity. The conductivity of In_2O_3 was strongly dependent on annealings in oxygen or vacuum, indicating that the native point defects oxygen vacancies and oxygen interstitials to play a major role as UID or compensating donors and compensating acceptors, respectively. The Seebeck coefficient and mobility of In_2O_3 as a function of electron concentration was measured and modeled [16]. Combined Hall and Seebeck measurements were able to prove the bulk character of our UID donors as opposed to surface donors.

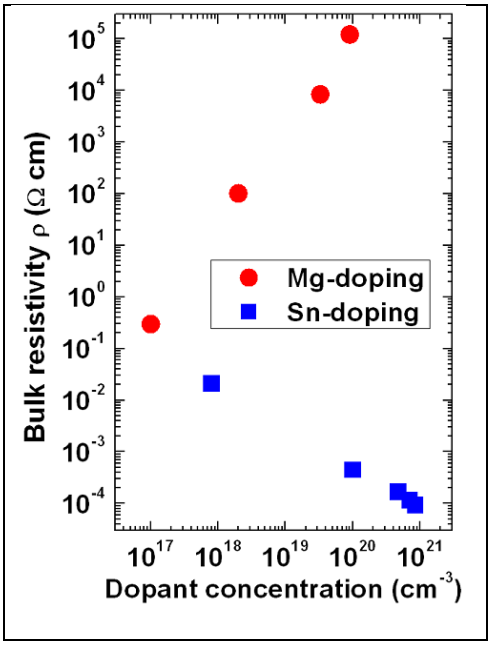

Fig. 2 Control of In_2O_3 resistivity by donor (Sn) and acceptor (Mg) doping.

References

[1] O. Bierwagen *et al.*"Chapter 15 - MBE of transparent semiconducting oxides" in "Molecular Beam Epitaxy" (2013) Elsevier Oxford.

[2] M.Y. Tsai *et al.*, J. Appl. Phys. **106** (2009) 024911.

[3] M.Y. Tsai *et al*., J. Vac. Sci. Technol. A **28** (2010) 354.

[4] O. Bierwagen *et al*., Appl. Phys. Lett. **95** (2009) 262105.

[5] O.Bierwagen and J.S. Speck, J. Appl. Phys. **107** (2010) 113519.

[6] M. White *et al*, J. Appl. Phys. **106** (2009) 093704.

[7] M. White *et al*, Appl. Phys. Express **3** (2010) 051101.

[8] O. Bierwagen et al., J. Mater. Res. **27** (2012) 2232.

[9] O. Bierwagen and J.S. Speck, Phys. Status Solidi A **211** (2014) 48.

[10] O. Bierwagen and J.S. Speck, Appl. Phys. Lett.**101** (2012) 102107.

[11] O. Bierwagen and J.S. Speck, Appl. Phys. Lett. **97** (2010) 072103.

[12] O. Bierwagen *et al*., Appl. Phys. Express **2** (2009) 106502.

[13] T. Nagata *et al*. J. Appl. Phys. **107** (2010) 033707.

[14] O. Bierwagen *et al*., Appl. Phys. Lett. **98** (2011) 172101.

[15] H. von Wenckstern *et al.*, APL Materials **2** (2014) 046104.

[16] N. Preissler *et al.*, Phys. Rev. B **88** (2013) 085305.